American Mineralogist, Volume 72, pages 29–38, 1987

Hydration of corundum-bearing xenoliths in the Qôrqut Granite Complex, Godthåbsfjord, West Greenland

MINIK T. ROSING,* DENNIS K. BIRD
Department of Geology, Stanford University, Stanford, California 94305, U.S.A.
ROBERT F. DYMEK
Department of Earth and Planetary Sciences, Washington University, and McDonnell Center for the Space Sciences, St. Louis, Missouri 63130, U.S.A.

ABSTRACT

Thermodynamic analysis of phase relations in a high-grade gneissic xenolith from the anatectic region of the late Archean Qôrqut Granite Complex indicates that fluids, probably derived from the granite complex, caused partial replacement of primary plagioclase, corundum, and biotite in the xenolith by epidote, margarite, and muscovite. Compositional relations within the metamorphic mineral assemblage, together with logarithmic activity and fugacity phase diagrams in the system Na_2O-K_2O-CaO-FeO-MgO-Fe_2O_3-Al_2O_3-SiO_2-H_2O, define local equilibrium constraints on temperature, oxygen fugacity, activity of aqueous silica, and cation activity ratios in the fluid phase during hydration of the xenolith.

The inferred lithostatic pressure at the time of intrusion of the granite complex is ~5 kbar. At this pressure and ~580°C, plagioclase and corundum react with water to form margarite. Equilibrium among plagioclase, corundum, margarite, biotite, epidote, muscovite, and an aqueous solution in the xenolith at this temperature and pressure requires an oxygen fugacity of $\sim 10^{-17}$ bars. At temperatures less than 580°C, the assemblage biotite + muscovite + margarite + epidote is stable over a wide range of cation to H^+ activity ratios and activity of silica in the fluid phase, but defines a narrow range of oxygen fugacities at any given temperature. The calculated oxygen fugacities for the xenolith are close to the maximum values estimated from Fe-Ti oxide phase relations in some granites and pegmatites reported in the literature. Hydration of plagioclase and corundum and the oxidation of biotite in the xenolith to form epidote, margarite, and muscovite require an influx of H_2O and possibly SiO_2 from the surrounding granite.

INTRODUCTION

The Qôrqut Granite Complex (QGC, Fig. 1) in southern West Greenland intruded high-grade polyphase gneisses during the late Archean (Burwell and Friend, 1979; Beech and Chadwick, 1980). A plagioclase-rich gneissic xenolith within the QGC, probably derived from the Malene supracrustal sequence, contains corundum and biotite that are partially replaced by margarite, epidote, and muscovite (Dymek, 1983). Dymek proposed that the textural and mineral-chemical features in the xenolith could be explained by oxidation of biotite and hydration of plagioclase and corundum to form epidote, muscovite, and margarite. The objective of this paper is to evaluate the thermodynamic constraints on the metamorphic and/or igneous fluid phase associated with this process. Thermodynamic analysis of phase relations in the system Na_2O-K_2O-CaO-FeO-MgO-Fe_2O_3-Al_2O_3-SiO_2-H_2O is used here to define local equilibrium constraints on the possible range of oxygen fugacities (f_{O_2}), cation activity ratios, and the activity of aqueous silica [$a_{SiO_2(aq)}$] in the xenoliths during the formation of the QGC.

Characterization of fluids associated with crustal anatexis and emplacement of deep-seated granite bodies may help in evaluating metasomatic redistribution of elements in the lower crust. In this case, we address a tectono-metamorphic event at 2600–2500 Ma characterized by the formation of anatectic granite bodies and by possible redistribution of alkalis and alkaline-earth elements near the late Archean amphibolite-granulite facies boundary in the craton of West Greenland (Moorbath et al., 1981).

THE QÔRQUT GRANITE COMPLEX

The Qôrqut Granite Complex (Fig. 1) is a suite of late Archean granites (2530 Ma) that were formed by at least three distinct intrusive phases including a late pegmatitic phase (McGregor, 1973; Pankhurst et al., 1973; Burwell and Friend, 1979; Brown and Friend, 1980a, 1980b; Brown et al., 1981). These granites intruded the Archean

* Present address: Geologic Museum, Oster Voldgade 10, DK-1350, Copenhagen, Denmark.

0003–004X/87/0102–0029$02.00

Fig. 1. Schematic geologic map of the Godthåbsfjord region of southern West Greenland. The circled star denotes the location of the corundum-bearing xenoliths in the QGC. ISB represents the location of the Isua supracrustal belt. The map is modified after Baadsgaard et al. (1984).

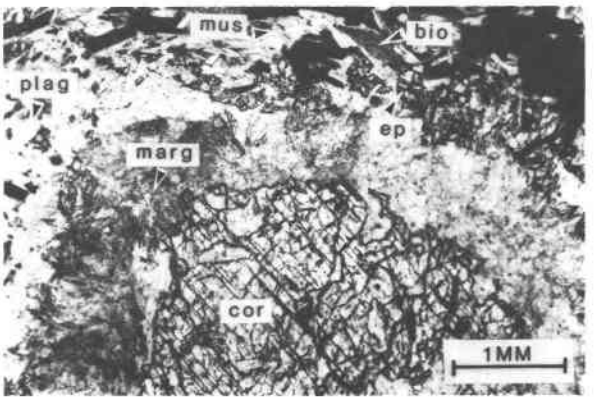

Fig. 2. Photomicrograph showing a reaction rim of margarite, muscovite, and epidote between a large corundum porphyroblast and the plagioclase and biotite matrix.

gneiss complex of West Greenland (Bridgwater et al., 1976), which consists of tonalitic-granitic orthogneisses with inclusions of meta-anorthositic and supracrustal lithologies. The currently exposed crustal level experienced granulite-facies metamorphism in the early Archean (3600 Ma, Griffin et al., 1980) and widespread amphibolite-facies and local granulite-facies metamorphism in the late Archean. Proterozoic metamorphism reached upper greenschist–lower amphibolite grade and involved considerable hydrothermal alteration in fault zones (Smith and Dymek, 1983; Rosing, 1984).

The age of the Qôrqut Granite Complex is bracketed by two metamorphic events: a 2800 Ma amphibolite-facies event and a less-pronounced upper greenschist–lower amphibolite facies event at ca. 2500 Ma (Baadsgaard, 1983). Lithostatic pressure at the time of intrusion of the granite is inferred to be ~5 kbar based on the crystallization sequence and fractionation trend of the QGC in the system SiO_2-$NaAlSi_3O_8$-$KAlSi_3O_8$-$CaAl_2Si_2O_8$ (Brown et al., 1981) and on the reconstructed metamorphic history of the Godthåbsfjord area (Fig. 1), which reveals that kyanite formed during penecontemporaneous regional retrograde metamorphism (Dymek, 1984). The xenolith studied here is from the lower portion of the QGC in which quartzofeldpathic gneisses with well-preserved banded structures are permeated by granitic bodies on a variety of scales ranging down to centimeter size, as detailed by Brown et al. (1981). It is likely, therefore, that the retrograde assemblage in the xenolith was strongly influenced if not controlled entirely by fluids associated with formation and subsequent crystallization of the granite.

Mineralogic phase relations and thermodynamic conventions

The petrology and mineral chemistry of this xenolith have been reported by Dymek (1983). As shown by the photomicrograph in Figure 2, it consists of large crystals of corundum (bright red; up to ~1 cm across), which are everywhere surrounded and replaced by mats of margarite (silvery in hand specimen; very pale brown in thin section). These corundum-margarite intergrowths are immersed in a matrix of finer-grained margarite, muscovite, biotite, and epidote ($X_{Ca_2Fe_3Si_3O_{12(OH)}} = 0.18$–$0.24$). Textures in the matrix indicate that the biotite is a relic phase that is replaced by the muscovite. Plagioclase ($X_{CaAl_2Si_2O_8} = 0.60$–0.80) is the most abundant phase in the xenolith and is partially replaced by epidote and/or margarite.

Representative compositions of the layer silicates from the xenolith are given in Table 1. The biotite has an exceptionally high Al content, indicating about 40% of the eastonite endmember, which is consistent with its former equilibrium coexistence with corundum in the xenolith. The muscovite contains only a small amount of paragonite component, but has a fairly high celadonite component, as revealed by low Na and modest (Fe,Mg) contents, respectively. Two analyses of margarite are listed in Table 1. The first corresponds to the coarser variety that immediately surrounds the corundum and is noteworthy for its high Na content, indicating about 20% paragonite component. The second margarite analysis given in Table 1 represents a fine-grained matrix margarite, which has a considerably lower paragonite content (~10%). A final feature worth noting is the exceedingly low F and Cl contents of the muscovite and margarite, as compared to biotite that contains up to ~0.3 wt% F and ~0.2 wt% Cl. This suggests, but does not prove, that the fluids responsible for the retrogression were probably poor in halogens.

Phase relations presented below were calculated using layer-silicate compositions reported in Table 1 (analyses 1 through 3) and the average compositions of plagioclase and epidote within the xenolith, together with equations and data describing the thermodynamic properties of minerals, water, ions, and gases reported by Helgeson et al. (1978), Helgeson and Kirkham (1974a, 1974b, 1976), Helgeson et al. (1981), Walther and Helgeson (1977),

Table 1. Mica compositions

	1	2	3	4
SiO_2	34.24	45.41	30.25	30.22
Al_2O_3	19.35	34.60	50.86	50.52
Cr_2O_3	0.05	0.03	0.04	0.05
TiO_2	1.21	0.20	0.05	0.02
MgO	10.00	0.83	0.21	0.09
FeO*	19.49	3.03	0.46	0.36
ZnO	0.08	0.00	0.00	0.00
MnO	0.23	0.00	0.01	0.00
CaO	0.24	0.22	11.86	12.38
BaO	0.09	0.10	0.03	0.01
Na_2O	0.13	0.42	1.34	0.79
K_2O	9.52	10.50	0.05	0.20
F	0.22	0.01	0.00	0.00
Cl	0.14	0.00	0.02	0.00
Total**	94.87	95.35	95.18	94.64
		O = 11		
Si	2.643	3.056	2.013	2.021
Al^{IV}	1.357	0.944	1.987	1.979
Al^{VI}	0.403	1.801	2.002	2.005
Cr	0.003	0.001	0.002	0.003
Ti	0.071	0.010	0.003	0.001
Mg	1.151	0.083	0.021	0.009
Fe	1.258	0.171	0.026	0.020
Zn	0.004	0.000	0.000	0.000
Mn	0.015	0.000	0.001	0.000
Ca	0.020	0.016	0.846	0.887
Ba	0.003	0.003	0.001	0.000
Na	0.019	0.055	0.173	0.102
K	0.937	0.901	0.004	0.017

Note: Columns are (1) biotite, (2) muscovite, (3) margarite (rim on corundum), and (4) margarite (matrix).
* All Fe as FeO.
** Less oxygen for F and Cl.

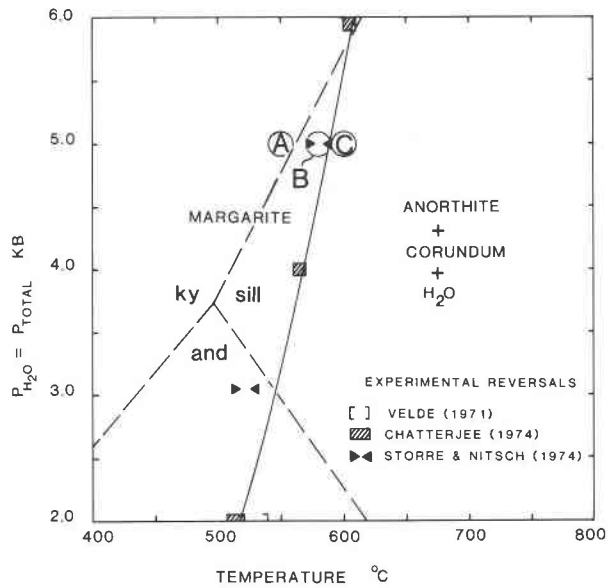

Fig. 3. Experimental reversals and univariant equilibrium curve for Reaction 1. Symbols A, B, and C denote the temperatures and pressures of the logarithmic activity-activity diagrams given in Figs. 4A, 4B, and 4C, respectively. Dashed lines denote phase relations among polymorphs of Al_2SiO_5 (and = andalusite, ky = kyanite, and sill = sillimanite). The curve is computed from equations and data reported by Helgeson et al. (1978) and Helgeson and Kirkham (1974a).

and Bird and Helgeson (1980). In this study, the thermodynamic activity of the $CaAl_2Si_2O_8$ component in plagioclase solid solutions was approximated by the activity-composition relations reported by Orville (1972). The activity of Al_2O_3 in corundum was assumed to be unity. Equations and data reported by Bird and Helgeson (1980) were used to evaluate the activities of the $Ca_2Al_3Si_3O_{12}(OH)$ and $Ca_2FeAl_2Si_3O_{12}(OH)$ components of epidote solid solutions. This mixing model explicitly accounts for the temperature dependence of substitutional order-disorder of Al^{3+} and Fe^{3+} in the M_1 and M_3 octahedral sites of epidote. Activities of margarite, biotite, and muscovite were calculated from equations and data reported by Aagaard and Helgeson (1983) and from assumed random mixing and equal interaction of atoms on energetically equivalent sites. The standard states adopted for the thermodynamic components $KMg_3(AlSi_3O_{10})(OH)_2$, $KFe_3(AlSi_3O_{10})(OH)_2$, and $KAl_2(AlSi_3O_{10})(OH)_2$ require that tetrahedral Al is ordered into the T_1O sites in biotite and muscovite (cf. Helgeson et al., 1978; Bird and Norton, 1981) and that tetrahedral Al in margarite is ordered in the two T_1 sites. Total analyzed Fe in biotite was considered to be FeO.

Activity and fugacity phase diagrams presented below define the mineralogic constraints on f_{O_2}, $a_{SiO_2(aq)}$, and cation to H^+ activity ratios in the fluid phase during oxidation and hydration of the xenolith. These phase diagrams were computed at the estimated pressure of 5 kbar for the QGC and represent the limiting condition where $a_{H_2O} = 1$. Although it is probable that high concentrations of electrolytes may have been present in the fluid phase associated with the retrograde alteration of the xenolith, a_{H_2O} is commonly close to unity in these solutions if they contain little or no dissolved CO_2 (Helgeson, 1967, 1969, 1980). Because the stability of zoisite and margarite in the system CaO-Al_2O_3-SiO_2-H_2O-CO_2 is restricted to fluids where $X_{CO_2} < 0.25$ at 5 kbar (Chatterjee, 1976; Allen and Fawcett, 1982), it is highly likely that the fluids responsible for the formation of epidote and margarite assemblages in the xenolith were water-rich.

Logarithmic ratios of the activities of cations (Na^+, Ca^{2+}, Mg^{2+}, Al^{3+}, and K^+) to H^+ are used here as descriptive variables in the phase diagrams (cf. Bowers et al., 1984). These dissociated cations are not necessarily the predominant species in the aqueous solution. In fact, evidence summarized by Quist and Marshall (1968), Helgeson (1969, 1980), Helgeson and Kirkham (1976), and Frantz and Marshall (1982) indicates that chloride complexes of the alkali and alkaline-earth cations will be the dominant aqueous species at 5 kbar and >500°C. At constant a_{H_2O}, the cation to H^+ activity ratios used here correspond to degrees of freedom in the Gibbs phase rule (Helgeson, 1970) and, together with equations and data reported by Helgeson and Kirkham (1976) and Helgeson et al. (1978, 1981), permit quantitative evaluation of solution-mineral equilibria at high pressures and temperatures.

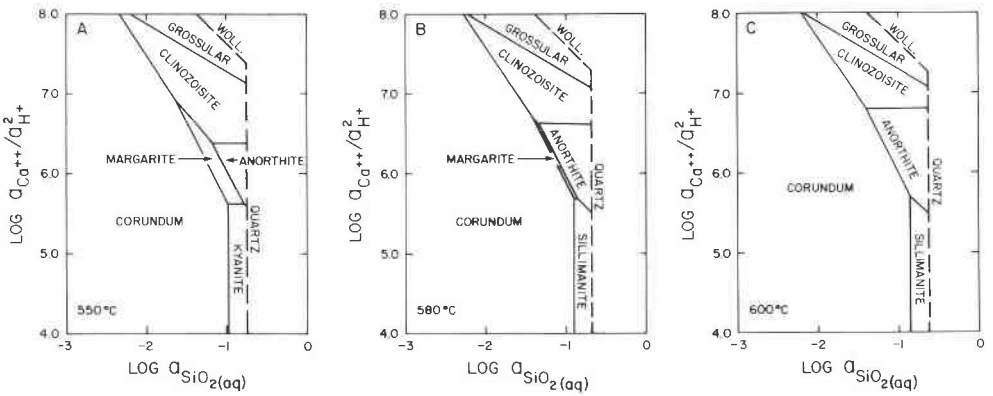

Fig. 4. Phase relations among stoichiometric minerals in the system CaO-Al_2O_3-SiO_2-H_2O in the presence of an aqueous solution in which $a_{H_2O} = 1$ as a function of log $a_{Ca^{2+}}/a_{H^+}$ and log a_{SiO_2} in the fluid phase at 550, 580, and 600°C and at 5 kbar (see Fig. 3). The dashed lines denote saturation in the fluid phase with either wollastonite or quartz.

Phase relations among stoichiometric minerals

The reaction of corundum, anorthite, and water to form margarite is well characterized experimentally (Velde, 1971; Chatterjee, 1974; Storre and Nitsch, 1974). Experimental reversals for this reaction between 2 and 6 kbar are shown in Figure 3 together with the calculated univariant curve for the reaction

$$\underset{\text{anorthite}}{CaAl_2Si_2O_8} + \underset{\text{corundum}}{Al_2O_3} + \underset{\text{fluid}}{H_2O} = \underset{\text{margarite}}{CaAl_2(Al_2Si_2O_{10})(OH)_2}. \quad (1)$$

Although this reaction can be used to evaluate the maximum temperature for formation of margarite in the xenoliths, little information is revealed about the nature of the aqueous solutions associated with hydration and oxidation of the high-grade metamorphic mineral assemblages.

To illustrate the stability relations of margarite, phase relations in the system CaO-Al_2O_3-SiO_2-H_2O are given in Figure 4 as a function of log $(a_{Ca^{2+}}/a^2_{H^+})$ and log $a_{SiO_2(aq)}$ in an aqueous solution at three temperatures (550, 580, and 600°C) and $P_{H_2O} = P_{total} = 5$ kbar. At 580°C, which is slightly below the equilibrium temperature of Reaction 1 (Fig. 4B), margarite is stable in a narrow field between corundum and anorthite that is characterized by a wide range in values of $a_{Ca^{2+}}/a^2_{H^+}$ and $a_{SiO_2(aq)}$ in the aqueous solution. With decreasing temperature (Fig. 4A), the stability field of margarite and clinozoisite expands, stabilizing both minerals with a broader range of activities of these aqueous species.

Values of log $a_{Ca^{2+}}/a^2_{H^+}$ and log $a_{SiO_2(aq)}$ in a fluid phase in equilibrium with corundum and other minerals in the system CaO-Al_2O_3-SiO_2-H_2O are shown in Figure 5 as a function of temperature. Equilibrium between the fluid phase and either sillimanite or kyanite defines the minimum values of $a_{Ca^{2+}}/a^2_{H^+}$ and the maximum $a_{SiO_2(aq)}$ in the fluid phase in equilibrium with margarite and corundum (Fig. 5). As a consequence of the small standard molal enthalpies of the reactions describing these phase boundaries (< -36 kJ/mol at 500°C and 5kbar), the logarithm of $a_{Ca^{2+}}/a^2_{H^+}$ and $a_{SiO_2(aq)}$ change only slightly with decreasing temperature between 587°C and 450°C. The maximum values of $a_{Ca^{2+}}/a^2_{H^+}$ and the minimum values of $a_{SiO_2(aq)}$ in the fluid phase in equilibrium with margarite + corundum are defined by the clinozoisite + corundum phase boundary. The activity of SiO_2(aq) in the aqueous solution in equilibrium with the assemblage margarite + clinozoisite + corundum decreases dramatically with decreasing temperature owing to the large positive standard molal enthalpy of the reaction characterizing this assemblage (104 kJ/mol at 500°C and 5 kbar). Values of $a_{Ca^{2+}}/a^2_{H^+}$ in equilibrium with this assemblage increase with decreasing temperature as a result of the large negative standard molal enthalpy of the reaction describing the margarite-clinozoisite phase boundary on the corundum saturation surface (-146 kJ/mol at 500°C and 5 kbar).

Solution-mineral equilibria in the QGC xenolith

Phase diagrams presented above for stoichiometric minerals and unit activity of H_2O (a_{H_2O}) permit evaluation of local equilibrium constraints of the metasomatic phase relations in the QGC xenolith. Of particular interest are equilibrium constraints imposed by the mineral compositions in the xenolith and the activity-composition relations adopted above for plagioclase$_{ss}$, margarite$_{ss}$, biotite$_{ss}$, muscovite$_{ss}$, and epidote$_{ss}$. The subscript "ss" is used here to denote the mineral compositions in the xenolith used in the calculations presented below which correspond to analyses 1 through 3 for micas in Table 1 and to the average compositions of plagioclase and epidote.

The maximum temperature of hydration of plagioclase and corundum to form margarite can be computed from the law of mass action for Reaction 1 and the activities of the components $CaAl_2Si_2O_8$ in plagioclase and of $CaAl_2(Al_2Si_2O_{10})(OH)_2$ in margarite from the xenolith. At 5 kbar and unit activity of water, the logarithm of the

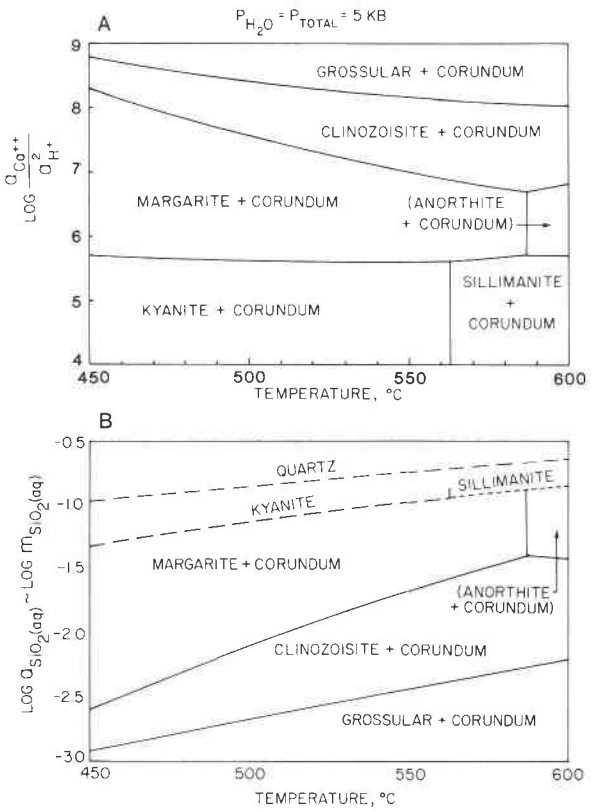

Fig. 5. Phase relations among stoichiometric minerals in the system CaO-Al_2O_3-SiO_2-H_2O in the presence of corundum and an aqueous solution in which $a_{H_2O} = 1$ as a function of temperature and log $a_{Ca^{2+}}/a_{H^+}$ and log $a_{SiO_2(aq)}$ in the fluid phase at 5 kbar. The dashed curves denote saturation in the fluid phase with either kyanite, sillimanite, or quartz. Corundum is stable with the fluid phase in diagram B only at values of log $a_{SiO_2(aq)}$ below kyanite or sillimanite saturation.

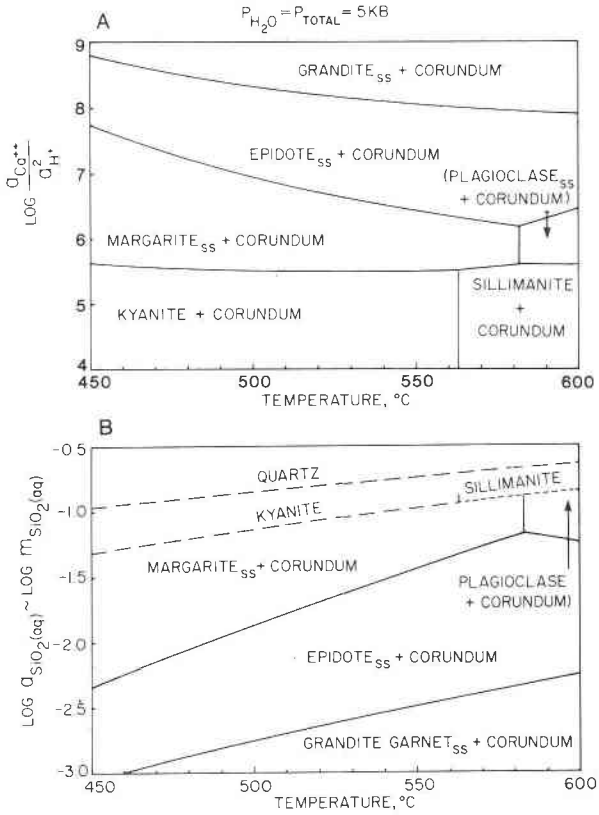

Fig. 6. Phase relations among nonstoichiometric minerals in the system Na_2O-CaO-Fe_2O_3-Al_2O_3-SiO_2-H_2O in the presence of corundum and an aqueous solution (see Fig. 5 caption). Mineral stabilities denote phase relations for the averaged compositions of metamorphic minerals within the plagioclase-rich gneissic xenolith of the QGC (see text).

activity product of Reaction 1 is -0.03, corresponding to an equilibrium temperature only ~ 10 deg lower than that for endmember compositions given in Figure 3.

In Figure 6, phase relations in the system Na_2O-CaO-Fe_2O_3-Al_2O_3-SiO_2-H_2O are given at 5 kbar for corundum saturation of the fluid phase. The stability field of epidote$_{ss}$ expands dramatically at the expense of plagioclase$_{ss}$ and margarite$_{ss}$ with introduction of the pistacite [$Ca_2Fe_3Si_3O_{12}(OH)$] component (cf. Figs. 5 and 6). The expanded epidote$_{ss}$ field causes the possible range of activities of aqueous species in equilibrium with the assemblage plagioclase$_{ss}$ + margarite$_{ss}$ + corundum to decrease relative to the stoichiometric mineral equilibria represented by Figures 3, 4, and 5. Substitution of Fe^{3+} for Al to form epidote$_{ss}$ requires an increased concentration of SiO_2(aq) but a decreased value of $a_{Ca^{2+}}/a^2_{H^+}$ in the fluid phase relative to the stoichiometric phase relations given in Figure 5.

Logarithmic activity-activity phase diagrams representing mineral stabilities for the compositions of epidote$_{ss}$, biotite$_{ss}$, muscovite$_{ss}$, plagioclase$_{ss}$, corundum, and margarite$_{ss}$ in the QGC xenolith are given in Figure 7 at 550°C and 5 kbar. Equilibrium among epidote$_{ss}$, margarite$_{ss}$, and an aqueous solution requires log $a_{SiO_2(aq)}$ values in the fluid phase between -1.0 and -1.5 and log $a_{Ca^{2+}}/a^2_{H^+}$ values between 5.95 and 6.5. Local equilibrium of this assemblage with corundum (point 1, Fig. 7A) determines the minimum concentration of SiO_2 and the maximum values of $a_{Ca^{2+}}/a^2_{H^+}$ and $a_{Al^{3+}}/a^3_{H^+}$ in the aqueous solution. The plagioclase$_{ss}$ + margarite$_{ss}$ + epidote$_{ss}$ assemblage shown by point 2 in Figure 7A represents the opposite extremes for the same fluid species.

Phase relations in the system Na_2O-K_2O-CaO-MgO-FeO-Fe_2O_3-Al_2O_3-SiO_2-H_2O are given in diagrams B and C of Figure 7 for the limiting case of corundum saturation (point 1, Fig. 7A). Points 3 and 4 in these diagrams denote values of log $a_{Ca^{2+}}/a^2_{H^+}$, log $a_{Mg^{2+}}/a^2_{H^+}$ and log a_{K^+}/a_{H^+} in an aqueous solution in equilibrium with biotite$_{ss}$, epidote$_{ss}$, margarite$_{ss}$, muscovite$_{ss}$, and corundum at 550°C and 5 kbar. The diagrams indicate that the activity of Ca^{2+} in the coexisting aqueous solution exceeds the activity of Mg^{2+} by several orders of magnitude. The calculated ratio of log $a_{Ca^{2+}}/a_{Mg^{2+}}$ varies from 2.35 for the limiting condition of corundum saturation (point 1, Fig. 7A and

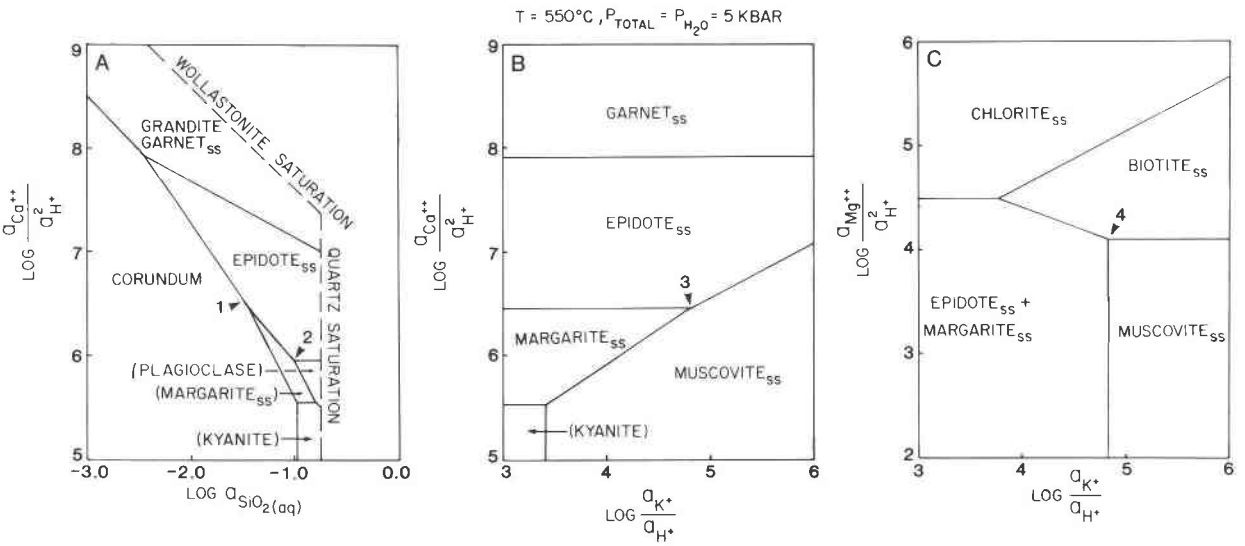

Fig. 7. Phase relations in the system Na_2O-K_2O-CaO-Fe_2O_3-Al_2O_3-SiO_2OH_2O where $a_{H_2O} = 1$. Diagrams B and C give phase relations in the presence of corundum. Mineral stabilities denote phase relations corresponding to compositions of metamorphic minerals within the plagioclase-rich xenolith of the QGC (see text).

point 3, Fig. 7C) to 1.93 for the plagioclase$_{ss}$-stable assemblage represented by point 2 in Figure 7A. The work by Frantz and Marshall (1982) indicates that the dissociation constants for $CaCl_2$ and $MgCl_2$ are similar. If the stoichiometric individual ion activity coefficients for Ca^{2+} and Mg^{2+} are also approximately equal, then the total concentration of Ca^{2+} in the fluid is approximately two orders of magnitude greater than Mg^{2+} for the conditions represented by the diagrams in Figure 7.

Local equilibrium constraints on the oxidation state of the system can be established from compositional relations among biotite$_{ss}$ and epidote$_{ss}$. The molar ratios of Al and Fe^{3+} in epidote$_{ss}$ and Fe^{2+} and Mg in biotite$_{ss}$ define f_{O_2} of the system as a function of pressure, temperature, and heterogeneous equilibria constraints on the chemical potentials of Al_2O_3 and MgO. In the xenolith, biotite is partially replaced by fine-grained muscovite and epidote. Local equilibrium of this assemblage with an aqueous solution can be represented by the reaction

$$4\underset{\text{annite}}{KFe_3(AlSi_3O_{10})(OH)_2} + 12\underset{\text{clinozoisite}}{Ca_2Al_3Si_3O_{12}(OH)} + 3O_2 + 12\underset{\text{fluid}}{H^+} = 4\underset{\text{muscovite}}{KAl_2(AlSi_3O_{10})(OH)_2} + 12\underset{\text{epidote}}{Ca_2FeAl_2Si_3O_{12}(OH)} + 4\underset{\text{fluid}}{Al^{3+}} + 6H_2O. \quad (2)$$

For constant mineral compositions, temperature, and pressure, the law of mass action for Reaction 2 requires $\log f_{O_2}$ to be a linear function of $\log a_{Al^{3+}}/a^3_{H^+}$ in the aqueous solution. Fixing $a_{Al^{3+}}/a^3_{H^+}$ by saturation of the fluid phase with corundum, the equilibrium represented by

$$4\underset{\text{annite}}{KFe_3(AlSi_3O_{10})(OH)_2} + 12\underset{\text{clinozoisite}}{Ca_2Al_3Si_3O_{12}(OH)} + \underset{\text{fluid}}{3O_2} = 4\underset{\text{muscovite}}{KAl_2(AlSi_3O_{10})(OH)_2} + 12\underset{\text{epidote}}{Ca_2FeAl_2Si_3O_{12}(OH)} + 2\underset{\text{corundum}}{Al_2O_3} \quad (3)$$

defines the f_{O_2}-temperature relations given by curve A–B in Figure 8 at 5 kbar. This curve describes the maximum f_{O_2} values for epidote$_{ss}$, biotite$_{ss}$, muscovite$_{ss}$, and an aqueous solution (see below). As noted above, substitution of Fe^{3+} in biotite$_{ss}$, is not accounted for in this study, but will increase slightly the predicted f_{O_2} represented by the curves given in Figure 8. The minimum f_{O_2} at temperatures >520°C at 5 kbar is constrained by the assemblage epidote$_{ss}$ + plagioclase$_{ss}$ + margarite$_{ss}$ + biotite$_{ss}$ + muscovite$_{ss}$ + aqueous solution. This equilibrium can be expressed as

$$4\underset{\text{annite}}{KFe_3(AlSi_3O_{10})(OH)_2} + 12\underset{\text{clinozoisite}}{Ca_2Al_3Si_3O_{12}(OH)} + 2\underset{\text{anorthite}}{CaAl_2Si_2O_8} + \underset{\text{fluid}}{2H_2O} + 3O_2 = 4\underset{\text{muscovite}}{KAl_2(AlSi_3O_{10})(OH)_2} + 12\underset{\text{epidote}}{Ca_2FeAl_2Si_3O_{12}(OH)} + 2\underset{\text{margarite}}{CaAl_2(Al_2Si_2O_{10})(OH)_2}, \quad (4)$$

which defines the $\log f_{O_2}$-temperature relations given by curve A–C in Figure 8. Point A denotes the temperature where Reactions 3 and 4 intersect at equilibrium defined by Reaction 1 (see Fig. 6). At 550°C and 5 kbar the corundum-stable (Reaction 3) and the plagioclase$_{ss}$-stable (Reaction 4) assemblages are represented by points 1 and 2 in Figure 7A, respectively. Point C in Figure 8 denotes the minimum equilibrium temperature for Reaction 4

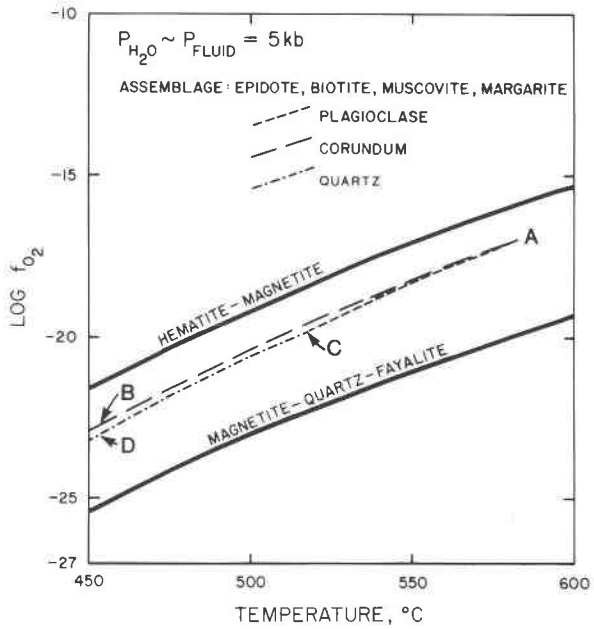

Fig. 8. Phase relations in the system Na_2O-K_2O-CaO-Fe_2O_3-Al_2O_3-SiO_2-H_2O-O_2 as a function of log f_{O_2} and temperature at 5 kbar. Curves A–B–C–D outline the area where epidote, biotite, muscovite, and margarite of the compositions from the QGC xenolith are stable at 5 kbar. This assemblage is in equilibrium with corundum along curve A–B, plagioclase along curve A–C, and quartz along curve C–D. See text.

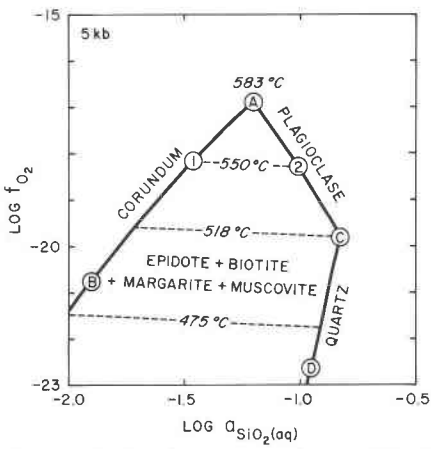

Fig. 9. Phase relations in the system Na_2O-K_2O-CaO-Fe_2O_3-Al_2O_3-SiO_2-H_2O-O_2 as a function of log f_{O_2} and log $a_{SiO_2(aq)}$ in the fluid phase at 5 kbar. The dashed lines represent constant-temperature equilibria involving epidote, biotite, muscovite, and margarite (Reaction 6). The solid lines denote equilibria of this assemblage with corundum (curve A–B), plagioclase (curve A–C), or quartz (curve C–D). Points 1 and 2 represent phase relations designated by points 1 and 2 in Fig. 7A. See Fig. 8.

defined by the hydration of plagioclase$_{ss}$ to form epidote$_{ss}$, margarite$_{ss}$, and quartz by the reaction

$$5\underset{\text{anorthite}}{CaAl_2Si_2O_8} + 2\underset{\text{fluid}}{H_2O} = 2\underset{\text{clinozoisite}}{Ca_2Al_3Si_3O_{12}(OH)} + \underset{\text{margarite}}{CaAl_2(Al_2Si_2O_{10})(OH)_2} + 2\underset{\text{quartz}}{SiO_2}. \quad (5)$$

Local equilibrium constraints of margarite$_{ss}$ on the f_{O_2} conditions of reactions involving epidote$_{ss}$, biotite$_{ss}$, and muscovite$_{ss}$ (i.e., phase boundary 1–2, Fig. 7A) can be written as

$$5\underset{\text{annite}}{KFe_3(AlSi_3O_{10})(OH)_2} + 16\underset{\text{clinozoisite}}{Ca_2Al_3Si_3O_{12}(OH)} + 3.75O_2 + \underset{\text{fluid}}{SiO_{2(aq)}} + 1.5H_2O = 5\underset{\text{muscovite}}{KAl_2(AlSi_3O_{10})(OH)_2} + 15\underset{\text{epidote}}{Ca_2FeAl_2Si_3O_{12}(OH)} + 2\underset{\text{margarite}}{CaAl_2Al_2Si_2O_{10}(OH)_2}. \quad (6)$$

For constant mineral compositions the law of mass action for Reaction 6 requires log f_{O_2} to be a linear function of log $a_{SiO_2(aq)}$ with a slope of -0.27. This relationship for epidote$_{ss}$, biotite$_{ss}$, muscovite$_{ss}$, and margarite$_{ss}$ equilibria in the xenolith at 550°C and 5 kbar is given by the dashed line (1–2) in Figure 9. This assemblage is in equilibrium with corundum at point 1 and with plagioclase$_{ss}$ at point 2 (compare with points 1 and 2 in Fig. 7A). Note that over the wide range of values of $a_{SiO_2(aq)}$ characterized by equilibrium epidote$_{ss}$ + margarite$_{ss}$ + muscovite$_{ss}$ + biotite$_{ss}$ (between points 1 and 2 in Fig. 9) that log f_{O_2} varies by only about 0.1. Also given in Figure 9 are the relationships of f_{O_2} and log $a_{SiO_2(aq)}$ for phase boundaries represented by curves A–B (Reaction 3) and A–C (Reaction 4) in Figure 8. Local equilibrium for the plagioclase$_{ss}$-bearing assemblage (curve A–C in Figs. 8 and 9) requires $a_{SiO_2(aq)}$ in the fluid phase to increase with decreasing temperatures until quartz saturation is reached at 518°C (point C, Fig. 9, and Reaction 5). Phase boundary C–D denotes equilibrium of Reaction 6 for saturation of the fluid phase with quartz.

The range of oxygen fugacities computed above for the assemblage epidote$_{ss}$ + margarite$_{ss}$ + muscovite$_{ss}$ + biotite$_{ss}$ is given in Figure 10 as a function of temperature at 5 kbar. Also shown in Figure 10 are predicted oxygen fugacities estimated from Fe-Ti oxide phase relations for a large number of granites and pegmatites reported in the literature. It is apparent from the phase relations given in Figure 10 that f_{O_2} in the xenolith was slightly higher than values characteristic of many granites.

Discussion

The mineral assemblages found in the xenolith are products of a series of events that led to the formation of the anatectic Qôrqut granite. Observed phase relations in the xenolith do not allow for explicit definition of the changes in chemical potentials of thermodynamic components associated with the oxidation and hydration of biotite, plagioclase, and corundum. However, the meta-

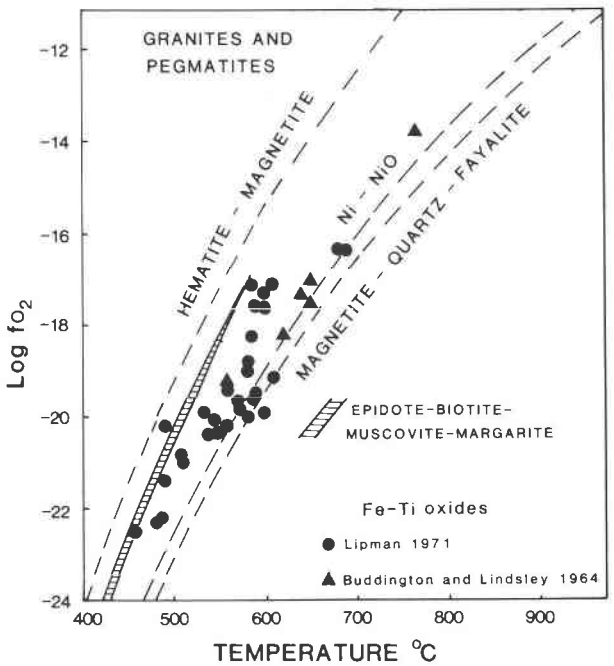

Fig. 10. Predicted $\log f_{O_2}$ and temperature conditions for the formation of retrograde mineral assemblages in plagioclase-rich xenoliths within the QGC (area defined by curves A–B–C–D; see Fig. 8) and of Fe-Ti oxides in granitic intrusions reported by Buddington and Lindsley (1964) and Lipman (1971). The solid curves represent equilibrium in the system FeO-Fe_2O_3-SiO_2 and Ni-NiO at 5 kbar.

morphic assemblages do allow for theoretical evaluation of several limiting cases for the condition that $a_{H_2O} \approx 1$. Three cases, defined by curves A–B, A–C, and C–D in Figure 9, represent the extremes of f_{O_2}, $a_{SiO_2(aq)}$, $a_{Ca^{2+}}/a^2_{H^+}$, and $a_{Al^{3+}}/a^3_{H^+}$ in the fluid phase in equilibrium with the assemblage epidote$_{ss}$ + margarite$_{ss}$ + biotite$_{ss}$ + muscovite$_{ss}$. These limiting cases correspond to local equilibrium of this assemblage with corundum, plagioclase$_{ss}$, or quartz at temperatures less than the hydration of plagioclase$_{ss}$ and corundum to form margarite$_{ss}$ at ~580°C and 5 kbar. Although epidote$_{ss}$, margarite$_{ss}$, biotite$_{ss}$, and muscovite$_{ss}$ can be in equilibrium over a wide range of $a_{SiO_2(aq)}$, this assemblage is stable only for a very narrow range in f_{O_2} at any given temperature (Figs. 8, 9, and 10).

In the plagioclase-rich xenoliths of the QGC, it is likely that the metamorphic and/or igneous fluids were close to equilibrium with plagioclase$_{ss}$ (An_{70}) at temperatures of >518°C. This would require $a_{SiO_2(aq)}$ to increase with decreasing temperature (curve A–C, Fig. 9), together with an increase in the chemical affinity between corundum and the aqueous solution resulting in the replacement of corundum by margarite$_{ss}$. At temperatures of <518°C, plagioclase$_{ss}$ in the xenolith will react with the aqueous solution along phase boundary C–D in Figure 9 to produce epidote and margarite, and possibly a more albite-rich plagioclase (Bird and Helgeson, 1981).

Oxidation of biotite (Reaction 6) and hydration of corundum (Reaction 1) to form epidote$_{ss}$, margarite$_{ss}$, and muscovite$_{ss}$ in the presence of plagioclase$_{ss}$ require transfer of H_2O and SiO_2(aq) from the H_2O-rich, quartz-saturated granitic melt into the corundum-bearing xenolith. It is apparent that the mass fluxes of SiO_2 and H_2O between the quartz-saturated granite and the xenolith were important processes during the formation of the xenolith's retrograde metamorphic assemblages. Although measurements have not been made, detailed field observations of compositional gradients within and near the xenolith in the QGC, together with the phase diagrams presented above, will provide a basis for description and interpretation of local metasomatic-element migration during anatexis in the lower crust.

The mineral assemblage biotite$_{ss}$ + epidote$_{ss}$ + muscovite$_{ss}$ + margarite$_{ss}$ is not a buffer sensu stricto since the phases are solid solutions that change composition with f_{O_2}. However, at constant a_{H_2O} the assemblage defines a narrow isobaric f_{O_2} range, as shown in Figures 8, 9, and 10. Like the oxygen-buffering capacity of the assemblage biotite, garnet, muscovite, magnetite, and quartz proposed by Zen (1985) for some peraluminous granites and metamorphic rocks, these types of assemblages can be used to constrain intensive thermodynamic variables in certain geologic systems.

Uncertainties associated with the thermodynamic calculations given above are complex and largely ambiguous functions of the errors in experimental observations and thermodynamic models for standard- and non-standard-state properties of the components and phases of the systems. Nevertheless, such calculations prove to be useful tools in the analysis of even complex geologic systems.

Acknowledgments

Critical reviews by Moonsup Cho, J. G. Liou, C. E. Manning, J. M. Rice, N. M. Rose, and J. V. Walther have greatly improved the content of this paper. Debbie Montgomery drafted a number of the figures. Bobbie Bishop, Halldora Hreggvidsdottir, and Chuck Karish are thanked for supportive and stimulating discussions.

Support from the Carlsberg Foundation and the Danish Natural Sciences Research Counsel, to M. Rosing, while a Visiting Scholar at Stanford is acknowledged. This research was supported in part by grant NSF-EAR 84-18129 to D.K.B.

References

Aagaard, P., and Helgeson, H.C. (1983) Activity/composition relations among silicates and aqueous solutions: II. Chemical and thermodynamic consequences of ideal mixing of atoms on homological sites in montmorillonites, illites, and mixed-layer clays. Clays and Clay Minerals, 31, 207–217.

Allen, J.M., and Fawcett, J.J. (1982) Zoisite-anorthite-calcite stability relations in H_2O-CO_2 fluids at 5000 bars: An experimental and SEM study. Journal of Petrology, 23, pt. 2, 215–239.

Baadsgaard, H. (1983) U-Pb isotope systematics on minerals from the gneiss complex at Isuakasia, West Greenland. Rapport Grønland Geologiske Undersøgelse, 112, 35–42.

Baadsgaard, H., Nutman, A.P., Bridgwater, D., Rosing, M., McGregor, V.R., and Allaart, J.H. (1984) The zircon geo-

chronology of the Akilia association and Isua supracrustal belt, West Greenland. Earth and Planetary Science Letters, 68, 221–228.

Beech, E.M., and Chadwick, B. (1980) The Malene supracrustal gneisses of northwest Buksefjorden: Their origin and significance in the Archaean crustal evolution of southern West Greenland. Precambrian Research, 11, 329–356.

Bird, D.K., and Helgeson, H.C. (1980) Chemical interaction of aqueous solutions with epidote-feldspar mineral assemblages in geologic systems. I. Thermodynamic analysis of phase relations in the system CaO-FeO-Fe_2O_3-Al_2O_3-SiO_2-H_2O-CO_2. American Journal of Science, 280, 907–941.

——— (1981) Chemical interaction of aqueous solutions with epidote-feldspar mineral assemblage in geologic systems. II. Equilibrium constraints in metamorphic/geothermal processes. American Journal of Science, 281, 576–614.

Bird, D.K., and Norton, D.L. (1981) Theoretical prediction of phase relations among aqueous solutions and minerals: Salton Sea geothermal system. Geochimica et Cosmochimica Acta, 45, 1479–1493.

Bowers, T.S., Jackson, K.J., and Helgeson, H.C. (1984) Equilibrium activity diagrams for coexisting minerals and aqueous solutions at pressures and temperatures to 5 kb and 600°C. Springer-Verlag, Berlin.

Bridgwater, D., Keto, L., McGregor, V.R., and Myers, J.S. (1976) The Archaean gneiss complex of Greenland. In A. Escher and W.S. Watt, Eds. Geology of Greenland. Grønlands Geologiske Undersøgelse, Copenhagen.

Brown, M., and Friend, C.R.L. (1980a) Field evidence concerning the origin of the early leucocratic granites within the Qôrqut granite complex in the area of Qôrqut. Rapport Grønlands Geologiske Undersøgelse, 100, 76–79.

——— (1980b) The polyphase nature and internal structure of the Qôrqut granite complex east of Umanap Suvdlua, Godthåbsfjord, southern West Greenland. Rapport Grønland Geologiske Undersøgelse, 100, 79–83.

Brown, M., Friend, C.R.L., McGregor, V.R., and Perkins, W.T. (1981) The late Archaean Qôrqut granite complex of southern West Greenland. Journal of Geophysical Research, 86, 10617–10632.

Buddington, A.F., and Lindsley, D.H. (1964) Iron-titanium oxide minerals and synthetic equivalents. Journal of Petrology, 5, 310–357.

Burwell, A.D.M., and Friend, C.R.L. (1979) Observations on the late Archaean Qôrqut granite, Qôrqut, Godthåbsfjord, southern West Greenland. Rapport Grønlands Geologiske Undersøgelse 95, 76–79.

Chatterjee, N.D. (1974) Synthesis and upper thermal stability of 2M margarite, $CaAl_2(Al_2Si_2O_{10})(OH)_2$. Schwiezerische Mineralogische und Petrographische Mitteilugen, 54, 753–767.

——— (1976) Margarite stability and compatibility relations in the system CaO-Al_2O_3-SiO_2-H_2O as a pressure-temperature indicator. American Mineralogist, 61, 699–709.

Dymek, R.F. (1983) Margarite pseudomorphs after corundum, Qôrqut area, Godthåbsfjord, West Greenland. Rapport Grønlands Geologiske Undersøgelse, 112, 95–99.

——— (1984) Supracrustal rocks, polymetamorphism, and evolution of the southwest Greenland Archean gneiss complex. In H.D. Holland and A.F. Trendall, Eds. Patterns of change in earth evolution, p. 313–343. Springer-Verlag, New York.

Frantz, J.D., and Marshall, W.L. (1982) Electrical conductances and ionization constanta of calcium chloride and magnesium chloride in aqueous solutions at temperatures to 600°C and pressure to 4000 bars. American Journal of Science, 282, 1666–1693.

Griffin, W.L., McGregor, V.R., Nutman, A.P., Taylor, P.N., and Bridgwater, D. (1980) Early Archaean granulite facies metamorphism south of Aneralik, West Greenland. Earth and Planetary Science Letters, 50, 59–74.

Helgeson, H.C. (1967) Solution chemistry and metamorphism. In P.H. Abelson, Ed. Researches in geochemistry, vol. 2, p. 362–404. Wiley, New York.

——— (1969) Thermodynamics of hydrothermal systems at elevated temperatures and pressures. American Journal of Science, 267, 729–804.

——— (1970) Description and interpretation of phase relations in geochemical processes involving aqueous solutions. American Journal of Science, 268, 415–438.

——— (1980) Prediction of the thermodynamic properties of electrolytes at high pressures and temperatures. In D.T. Rickard and F. Wickman, Eds. Chemistry and geochemistry of solutions at high temperatures and pressures: Physics and chemistry of the earth, 13–14, 133–177. Pergamon, New York.

Helgeson, H.C., and Kirkham, D.H. (1974a) Theoretical prediction of the thermodynamic behavior of aqueous electrolytes at high pressures and temperatures. I. Summary of the thermodynamic/electrostratic properties of the solvent. American Journal of Science, 274, 1089–1198.

——— (1974b) Theoretical prediction of the thermodynamic behavior of aqueous electrolytes at high pressures and temperatures. II. Debye-Hückel parameters for activity coefficients and relative partial molal properties. American Journal of Science, 274, 1199–1261.

——— (1976) Theoretical prediction of the thermodynamic behavior of aqueous electrolytes at high pressures and temperatures. III. Equation of state for aqueous species at infinite dilution. American Journal of Science, 276, 97–240.

Helgeson, H.C., Delany, J.M., Nesbitt, H.W., and Bird, D.K. (1978) Summary and critique of the thermodynamic properties of rock-forming minerals. American Journal of Science, 278A, 229 p.

Helgeson, H.C., Kirkham, D.H., and Flowers, G.C. (1981) Theoretical prediction of the thermodynamic behavior of aqueous electrolytes at high pressures and temperatures. IV. Calculation of activity coefficients, osmotic coefficients and apparent molal and standard and relative partial molal properties to 600°C and 5 kb. American Journal of Science, 281, 1249–1516.

Lipman, P.W. (1971) Iron-titanium oxide phenocrysts in compositionally zoned ash-flow sheets from southern Nevada. Journal of Geology, 79, 438.

McGregor, V.R. (1973) The early Precambrian gneisses of the Godthåb district, West Greenland. Royal Society of London Philosophical Transactions, A273, 343–358.

Moorbath, S., Taylor, P.N., and Goodwin, R. (1981) Origin of granitic magma by crustal remobilisation: Rb-Sr and Pb/Pb geochronology and isotope geochemistry of the late Archaean Qôrqut granite complex of southern West Greenland. Geochimica et Cosmochimica Acta, 45, 1051–1060.

Orville, P.M. (1972) Plagioclase cation exchange equilibria with aqueous chloride solution: Results at 700°C and 2000 bars in the presence of quartz. American Journal of Science, 272, 234–272.

Pankhurst, R.J., Moorbath, S., Rex, D.C., and Turner, G. (1973) Mineral age patterns in the c. 3700 my old rocks from West Greenland. Earth and Planetary Science Letters, 20, 157–170.

Quist, A.S., and Marshall, W.L. (1968) Electrical conductances of aqueous sodium chloride solutions from 0 to 800° and at pressures to 4000 bars. Journal of Physical Chemistry, 72, 684–703.

Rosing, M. (1984) Metamorphic and isotopic studies of the Isua supracrustals, West Greenland. Unpublished Cand. Scient. thesis, Copenhagen University, Copehagen, Denmark.

Smith, G.M., and Dymek, R.F. (1983) A description and interpretation of the Proterozoic Kobbefjord fault zone, Godthåb District, West Greenland. Rapport Grønlands Geologiske Undersøgelse, 112, 113–127.

Storre, B., and Nitsch, K.H. (1974) Zur stabilität von Margarit im system CaO-Al_2O_3-SiO_2-H_2O. Contributions to Mineralogy and Petrology, 43, 1–24.

Velde, B. (1971) The stability and natural occurrence of margarite. Mineralogical Magazine, 38, 317–323.
Walther, J.V., and Helgeson, H.C. (1977) Calculation of the thermodynamic properties of aqueous silica and the solubility of quartz and its polymorphs at high pressures and temperatures. American Journal of Science, 277, 1315–1351.
Zen, E. (1985) An oxygen buffer for some peraluminous granites and metamorphic rocks. American Mineralogist, 70, 65–73.

Manuscript received July 24, 1985
Manuscript accepted September 2, 1986